Polyhedron 30 (2011) 1375–1384

Contents lists available at ScienceDirect

Polyhedron

journal homepage: www.elsevier.com/locate/poly

Dioxo- and oxovanadium(V) complexes of biomimetic hydrazone ONO and NNS donor ligands: Synthesis, crystal structure and catalytic reactivity

Hassan Hosseini Monfared [a,*], Samaneh Kheirabadi [a], Nasim Asghari Lalami [a], Peter Mayer [b]

[a] Department of Chemistry, Zanjan University, 45195-313 Zanjan, Iran
[b] Fakultät für Chemie und Pharmazie, Ludwig-Maximilians-Universität, München, Butenandtstr. 5-13, Haus D, D-81377 München, Germany

ARTICLE INFO

Article history:
Received 4 December 2010
Accepted 3 February 2011
Available online 17 February 2011

Keywords:
Methoxy-bridged vanadium complex
Hydrazone complexes
Crystal structure
Catalytic activity
Proton-transfer complex

ABSTRACT

Oxo- and dioxo-vanadium(V) complexes of hydrazone ONO donor ligands with the formula $[V^{V}O(\mu_2\text{-}OCH_3)(L^1)]_2$ (**1**) and $[V^{V}O_2(L^2)]\cdot H_2O$ (**2**) were synthesized by the reaction of $[VO(acac)_2]$ with proton-transfer complexes of benzenetricarboxylic acid/benzoylhydrazide and benzenetricarboxylic acid/isonicotinohydrazide, respectively (H_2L^1 = monocondensation of benzoylhydrazide and acetylacetone, H_2L^2 = monocondensation of isonicotinohydrazide and acetylacetone). Dioxo complex of V(V), $[VO_2(L^3)]$ (**3**), was synthesized by the reaction of equimolar amounts of $VO(acac)_2$, 2-acetylpyridine and thiosemicarbazide (H_2L^3 = hydrazone Schiff base of acetylpyridine and thiosemicarbazide and Hacac = acetylacetone). They were characterized by FT-IR, UV–Vis and NMR spectroscopic methods. The crystal structures of **1** and **2** were determined by X-ray analyses. The ^1H NMR spectrum of the complex **1** in $CDCl_3$ solution indicated that this dimeric complex is converted appreciably into its respective monomeric form. The catalytic potential of the complexes has been tested for the oxidation of alkene, alkane and aromatic hydrocarbons using H_2O_2 as the terminal oxidant. Good to excellent conversions have been obtained for the oxidation of most of the hydrocarbons.

1. Introduction

The coordination chemistry of vanadium has received considerable attention since the discovery of vanadium in the vanadium-dependent haloperoxidases [1,2], nitrogenases [3] and nitrate reductases [4]. The structures and properties of these vanadium enzymes have stimulated the search for structural and functional model compounds [5–8]. Oxovanadium(IV) and dioxovanadium(V) complexes with N-, O- and S-donor chelating ligands have been studied for their potential insulin-mimetic effects [9,10], tumor growth inhibition and prophylaxis against carcinogenesis [11], to inhibit several enzymes, including phosphatases, ATPases, nucleases, kinases [12] and the antimicrobial activity against *Mycobacterium tuberculosis* [13].

On the other hand, hydrazones —NH—N=CRR′ (R and R′ = H, alkyl, aryl) are versatile ligands due to their applications in the field of analytical [14] and medicinal chemistry [15]. Hydrazones exhibit physiological activities in the treatment of several diseases such as tuberculosis. This activity is attributed to the formation of stable chelate complexes with transition metals which catalyze physiological processes [16]. Hydrazone moieties are the most important pharmacophoric cores of several antiinflammatory, antinociceptive, and antiplatelet drugs [17]. The biological profile of compounds presenting this subunit is related to its relative acidity and its capacity to stabilize free radicals [18]. It has been found that oxovanadium(IV) and *cis*-dioxovanadium(V) complexes of thiosemicarbazone show comparable or larger anti-*M. tuberculosis* activities than the free thiosemicarbazone ligands [19].

The use of oxovanadium complexes in oxidation and oxotransfer catalysis has been noted [20]. Various organic substrates are oxidized by peroxides in the presence of vanadium and dioxovanadium(V) complexes [21,22]. Dioxovanadium(V) complexes are commonly synthesized (i) by the reaction of vanadates with ONO-functional ligands in aqueous solution [23,24]; (ii) by the reaction of triethyl vanadate, $[VO(OEt)_3]$, with appropriate ligands [25] or (iii) by oxidation of oxovanadium(IV) complexes with KNO_2 in H_2O/MeOH [26] and (iv) by the reaction of $[VO(acac)_2]$ (acacH = acetylacetone) or $VOSO_4$ with the ligands in non-aqueous or mixed solvent media followed by oxidation with O_2 [5,27]. To the best of our knowledge there is no report on the synthesis of neutral dioxovanadium(V) complexes of hydrazone ligands via proton-transfer complexes.

In view of importance of vanadium compounds, and also extending the search for more efficacious compounds of vanadium with neutral charge (one of the desirable qualities of vanadium compounds to be useful as biomimetic drugs include neutral charge [28]), we present here the synthesis and characterization of oxovanadium(V) and dioxovanadium complexes of the hydrazones H_2L^1, H_2L^2 and HL^3 derived from acetylacetone/

* Corresponding author. Tel.: +98 241 5152576; fax: +98 241 5283203.
E-mail address: monfared@znu.ac.ir (H. Hosseini Monfared).

0277-5387/$ - see front matter © 2011 Elsevier Ltd. All rights reserved.
doi:10.1016/j.poly.2011.02.005

benzoylhydrazide, acetylacetone/isonicotinohydrazide and acetylpyridine/thiosemicarbazide; Scheme 1. Neutral oxo and dioxovanadium(V) complexes of hydrazone ligands were synthesized via proton-transfer complexes. As many vanadium complexes show catalytic activity in oxidation and oxygen transfer reactions [29], including the oxidation of (prochiral) organic sulfides to (chiral) sulfoxides [30], thus modeling the haloperoxidase activity, related reactivity patterns have also been studied by testing the catalytic activity of the complexes with respect to the oxidation of hydrocarbons using H_2O_2 as an oxidant.

2. Experimental

Bis(acetylacetonato)oxovanadium(IV), $[VO(acac)_2]$, alkenes, solvents and other materials with high purity were purchased from Merck and Fluka and used as received. IR spectra were recorded as KBr disks with a Matson 1000 FT-IR spectrophotometer in the range of 4000–450 cm^{-1}. UV–Vis spectra of solution were recorded on a Shimadzu 160 spectrometer. ^1H NMR spectra in DMSO-d^6 solution were recorded on a Bruker 250 MHz spectrometer and chemical shifts are indicated in ppm relative to tetramethylsilane. The reaction products of oxidation were determined and analyzed by HP Agilent 6890 gas chromatograph equipped with a HP-5 capillary column (phenyl methyl siloxane 30 m × 320 μm × 0.25 μm) and gas chromatograph–mass spectrometry (Hewlett-Packard 5973 Series MS-HP gas chromatograph with a mass-selective detector). The elemental analyses (carbon, hydrogen, and nitrogen) of compounds were obtained from Carlo ERBA Model EA 1108 analyzer. Vanadium percentages of complexes were measured by a Varian spectrometer AAS-110.

2.1. Synthesis of $[HBzh^+]_3[BTC^{3-}]$

At first the benzoylhydrazide–benzenetricarboxylic acid proton-transfer complex ($[HBzh^+]_3[BTC^{3-}]$) was prepared. For the synthesis of $[HBzh^+]_3[BTC^{3-}]$, a mixture of benzoylhydrazide (Bzh) (0.38 g, 2.79 mmol) and benzene-1,3,5-tricarboxylic acid (H_3BTC) (0.20 g, 0.95 mmol) in methanol (10 ml) was refluxed for 5 h. The white crystalline precipitate of proton-transfer complex ($[HBzh^+]_3[BTC^{3-}]$) obtained on cooling the reaction media was filtered, washed with methanol and dried in air. Yield: 34% (199 mg). ^1H NMR (250.13 MHz, $CDCl_3$): δ = 3.49 (s (sharp), 3H, NH_3^+), 7.26–7.51 (m, 5H, benzoylhydrazide aryl), 7.86 (d, 3H, BTC^{3-} aryl), 8.46 (s (broad), 1H, amid —NH—).

2.2. Synthesis of $[V^VO(\mu_2\text{-}OCH_3)(L^1)]_2$ (**1**)

To a solution of $[Bzh^+]_3[BTC^{3-}]$ (119 mg, 0.19 mmol) in methanol (15 ml), $[VO(acac)_2]$ (50 mg, 0.19 mmol) was added. The reaction mixture was stirred under reflux for 4 h. The obtained black colored mixture was cooled to room temperature and the product $[V^VO(\mu_2\text{-}OCH_3)(L^1)]_2$ was removed by filtration, washed with methanol and dried in air. Yield: 95% (113 mg). X-ray quality crystals of $[V^VO(\mu_2\text{-}OCH_3)(L^1)]_2$ could be grown from methanol. *Anal.* Calc. for $C_{26}H_{30}N_4O_8V_2$ (628.42): C, 49.69; H, 4.81; N, 8.92; V, 16.21. Found: C, 49.45; H, 4.61; N, 9.00; V, 16.10%. IR (KBr, cm^{-1}): 3457 (m, br), 2924 (m), 2856 (w), 1718 (w), 1600 (m), 1547 (s), 1495 (m), 1390 (s), 1276 (m), 1033 (m), 980 (s), 944 (m), 895 (w), 785 (m), 698 (m), 596 (s), 499 (m). ^1H NMR (250.13 MHz, $CDCl_3$): δ = 1.92 (s, 3H, 3×H-8(bridged)), 2.30 (s, 3H, 3×H-12(bridged)), 2.42 (s, 3H, 3×H-8, monomer), 2.56 (s, 3H, 3×H-12, monomer), 3.49 (s, 3H, V-OCH_3, monomer), 5.12 (s, 3H, OCH_3 (bridged)), 5.52 (s, 1H, H-10, monomer), 5.71 (s, 1H, H-10 (bridged)), 7.21–8.10 (m, 5H, aryl (monomer and dimmer)). λ_{max} (ε, $dm^3\ mol^{-1}\ cm^{-1}$) = 214 (52 500), 271 (8700), 345 nm (4250).

2.3. Synthesis of $[H_2Inh^{2+}][HBTC^{2-}]$

For the synthesis of the isonicotinohydrazide–benzenetricarboxylic acid proton-transfer complex ($[H_2Inh^{2+}][HBTC^{2-}]$), a mixture of isonicotinohydrazide (Inh) (40 mg, 0.29 mmol) and benzene-1,3,5-tricarboxylic acid (BTC) (20 mg, 0.10 mmol) in methanol (10 ml) was refluxed for 4 h. The white crystalline precipitate of proton-transfer complex ($[H_2Inh^{2+}][HBTC^{2-}]$) obtained on cooling the reaction media was filtered, washed with methanol and dried in air. Yield: 32% (25 mg). ^1H NMR (250.13 MHz, $CDCl_3$): δ = 3.49 (very broad, 3H, NH_3^+), 4.20 (very broad, 1H, pyridinium-NH^+), 7.26–7.60 (m, 4H, aromatic of Inh), 7.72 (s, 3H, BTC^{3-}), 8.78 (s, 1H, amid —NH—).

2.4. Synthesis of $[V^VO_2(L^2)]\cdot H_2O$ (**2**)

To a solution of $[H_2Inh^{2+}][HBTC^{2-}]$ (84 mg, 0.10 mmol) in methanol (10 ml), $[VO(acac)_2]$ (60 mg, 0.23 mmol) was added. The

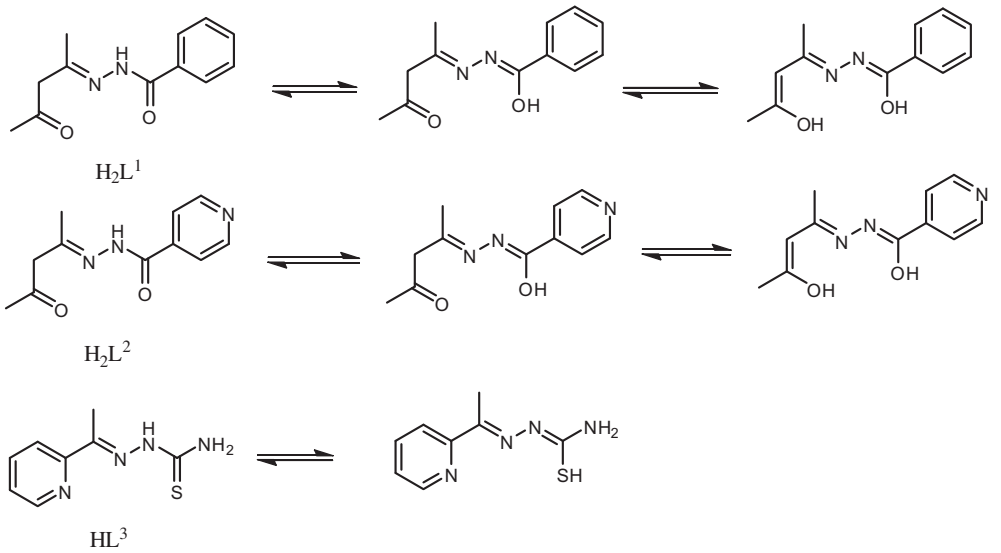

Scheme 1. The ligands H_2L^{1-2} and HL^3 tautomerism.

reaction mixture was stirred under reflux for 5 h. The obtained black colored mixture was cooled to room temperature and $[V^{V}O_2(L^2)]\cdot H_2O$ was removed by filtration, washed with methanol and dried in air. Yield: 90% (66 mg). *Anal.* Calc. for $C_{11}H_{14}N_3O_5V\cdot H_2O$ (319.19): C, 41.39; H, 4.42; N, 13.16; V, 15.96. Found: C, 41.41; H, 4.39; N, 13.15; V, 16.10%. IR (KBr, cm^{-1}): 3450 (br, s, H_2O), 3088 (w), 2925(s), 2854 (s), 1719 (m), 1618 (m), 1589 (m), 1534 (m), 1492 (vs) 1399 (vs), 1290 (w), 1215 9w), 1030 (s), 997 (s), 859 (m), 689 (m), 479 (s), 443 (s). ^{1}H NMR (250.13 MHz, $CDCl_3$): δ = 2.50 (s, 3H, 3×H-5), 2.68 (s, 3H, 3×H-1), 8.50 (s, 2H, pyridinium) and 8.80 (s, 2H, pyridinium). ^{1}H NMR (250.13 MHz, DMSO-d^6): δ = 5.35 (s, 1H, H-3), 8.02 (s, 2H, pyridinium), 8.71 (s, 2H, pyridyl). λ_{max} (ε, $dm^3\ mol^{-1}\ cm^{-1}$) = 208 (38 800), 274 (12 300) and 354 nm (2650).

2.5. Preparation single crystals of $[V^{V}O_2(L^2)]\cdot H_2O$ (2)

The charge transfer complex $[Inh^{2+}]_3[BTC^{3-}]_2$ (14 mg, 16 mmol) and $[VO(acac)_2]$ (20.0 mg, 0.075 mmol) were placed in the main arm of the branched tube ('branched tube' method). A mixture of ethanol and water (50:50 v/v, 13 ml) was carefully added to fill the arms, the tube was sealed and the reagents containing arm immersed in an oil bath at 60 °C while the other arm was kept at ambient temperature. After 1 week, red-brown crystals were deposited in the cooler arm, which were filtered off, washed with methanol and air dried. Yield: 87% (21 mg).

2.6. Synthesis of 2-(1-(pyridin-2-yl)ethylidene)hydrazinecarbothioamide, HL^3

The ligand HL^3 was synthesized as described in the literature [31]. Yield: 93% (180 mg). *Anal.* Calc. for $C_8H_{10}N_4S$ (194.26): C, 49.46; H, 5.19; N, 28.84. Found: C, 49.43; H, 5.22; N, 28.83. ^{1}H NMR (250.13 MHz, DMSO-d^6): δ = 2.33 (s, 3H, CH_3), 7.30–8.52 (m, 4H, pyridyl), 8.10 (s, NH_2), 10.27 (s, 1H, NH). λ_{max} (ε, $dm^3\ mol^{-1}\ cm^{-1}$) = 201 (104 300), 314 nm (57 900).

2.7. Synthesis of $[VO_2(L^3)]$

$[VO_2(L^3)]$ was also synthesized by branched tube method from equimolar reaction of $[VO(acac)_2]$ with HL^3 in methanol. After 4 days, needle brown crystals were deposited in the cooler arm, which were filtered off, washed with methanol and air dried. Yield: 81% (79 mg). *Anal.* Calc. for $C_8H_9N_4O_2SV$ (276.19): C, 34.79; H, 3.28; N, 20.29; V, 18.44. Found: C, 34.70; H, 3.28; N, 20.22; V, 18.41%. IR (KBr, cm^{-1}): 3304 (m), 3145 (m), 1638 (s) (C=N), 1598 (m), 1553 (m), 1504 (m), 1448 (vs), 1373 (m), 1325 (m), 1185 (s), 1043 (w, V=O), 938 (vs, V=O), 883 (m), 810 (m), 775 (m), 741 (m), 621 (m), 473 (m). ^{1}H NMR (250.13 MHz, DMSO-d^6): δ = 2.50 (s, 3H), 7.57–8.62 (m, 4H, pyridyl), 7.81 (s, 2H, NH_2). λ_{max} (ε, $dm^3\ mol^{-1}\ cm^{-1}$) = 210 (64 700), 312 (54 000), 420 nm (2900). The crystal structure of **3** has been reported recently [19].

2.8. X-ray structure determination

Single crystals of **1** and **2** were carefully selected under a polarizing microscope. X-ray quality crystals of $[V^{V}O(\mu_2\text{-}OCH_3)(L^1)]_2$, (**1**) (brown) could be grown from methanol. Dark brown crystals of **1** (0.22 mm × 0.20 mm × 0.19 mm) and **2** (0.26 mm × 0.15 mm × 0.10 mm) were investigated in diffraction experiments at 200(2) K or 173(2) K on an Oxford XCalibur/a KappaCCD diffractometer and with monochromated Mo Kα radiation (λ = 0.71073). The structures were solved by Direct Methods with SIR97 [32], and refined with full-matrix least-squares techniques on F^2 with SHELXL-97 [33]. The crystal data and refinement parameters are presented in Table 1. The C-bonded hydrogen atoms were calculated in idealized geometry riding on their parent atoms. The O-bonded hydrogen atoms were located from the difference map and refined freely. Graphics were drawn with DIAMOND [34].

2.9. Experimental set up for catalytic oxidation

The liquid phase catalytic oxidations were carried out under air (atmospheric pressure) in a 25 ml round bottom flask equipped with a magnetic stirrer and immersed in a thermostated oil bath. In a typical experiment, H_2O_2 (3 mmol) was added to a flask containing the catalyst **1**, **2** or **3** (about 3 μmol) and a representative alkene, namely cyclooctene (1 mmol) in a solvent (2 ml). The course of the reaction was monitored using a gas chromatograph equipped with a capillary column and a flame ionization detector. The oxidation products were identified by comparing their retention times with those of authentic samples or alternatively by ^{1}H NMR and GC–mass analyses. Yields based on the added substrate were determined by a calibration curve. Control reactions were carried out in the absence of catalyst, under the same conditions as the catalytic runs. No products were detected.

3. Results and discussion

The ligands H_2L^1 and H_2L^2 were synthesized in situ and coordinated to vanadium by refluxing the proton-transfer complex of the corresponding hydrazide with $[VO(acac)_2]$. The proton-transfer complexes $[Bhz^+]_3[BTC^{3-}]$ and $[H_2Inh^{2+}][HBTC^{2-}]$ were obtained by direct reaction of benzene-1,3,5-tricarboxylic acid (H_3BTC) with

Table 1
Crystal data and structure refinement for $[V^{V}O(\mu_2\text{-}OCH_3)(L^1)]_2$ (**1**) and $[V^{V}O_2(L^2)]\cdot H_2O$ (**2**).

Compound	$[V^{V}O(\mu_2\text{-}OCH_3)(L^1)]_2$ (**1**)	$[V^{V}O_2(HL^2)]\cdot H_2O$ (**2**)[a]
Net formula	$C_{26}H_{30}N_4O_8V_2$	$C_{11}H_{14}N_3O_5V$
M_r (g mol^{-1})	628.422	319.188
T (K)	200(2)	173(2)
Crystal system	orthorhombic	orthorhombic
Space group	*Pbca*	*Pnma*
a (Å)	10.8712(3)	13.9893(6)
b (Å)	12.1990(3)	6.6960(4)
c (Å)	21.1367(6)	13.8666(8)
α (°)	90	90
β (°)	90	90
γ (°)	90	90
V (Å^3)	2803.10(13)	1298.92(12)
Z	4	4
D_{calc} (g cm^{-3})	1.48911(7)	1.63222(15)
μ (mm^{-1})	0.722	0.787
Absorption correction	'multi-scan'	'multi-scan'
Transmission factor range	0.92394–1.00000	0.96070–1.00000
Reflections measured	12 786	3366
R_{int}	0.0301	0.0268
Mean $\sigma(I)/I$	0.0370	0.0392
θ Range	4.22–26.33	4.21–26.31
Observed reflections	2086	1082
x, y (weighting scheme)	0.0493, 0	0.0422, 0
Hydrogen refinement	constr.	mixed
Reflections in refinement	2848	1433
Parameters	184	125
Restraints	0	2
$R(F_{obs})$	0.0296	0.0307
$R_w(F^2)$	0.0799	0.0793
S	0.937	0.985
Shift/error$_{max}$	0.001	0.001
Maximum electron density (e Å^{-3})	0.281	0.309
Minimum electron density (e Å^{-3})	−0.326	−0.337

[a] C-bound H: constr., O-bound H: distance fixed to 0.82 Å with U(H) = 1.5 U(O), N-bound H: distance fixed to 0.86 Å with U(H) = 1.2 U(N).

benzoylhydrazide (Bzh) and isonicotinohydrazide (Inh) in methanol, respectively. Reaction of $[VO(acac)_2]$ with $[Bhz^+]_3[BTC^{3-}]$ led to the condensation of benzoylhydrazide with one of the acetylacetonato groups and formation of $[V^VO(\mu_2\text{-}OCH_3)(L^1)]_2$ (**1**) (where H_2L^1 = Schiff base derived from monocondensation of acetylacetone and benzoylhydrazide). For the synthesis of complex $[V^VO_2(L^2)]\cdot H_2O$ (**2**) a method similar to complex **1** was followed but a dioxovanadium(V) complex was formed. All the stated reactions can be represented as Schemes 2 and 3 for complexes **1** and **2**. Complex **3** was formed in a straightforward fashion from solutions of the respective ligand (HL^3) and $[VO(acac)_2]$. The oxidizing agent for the formation of pentavalent state of vanadium is the aerial oxygen.

3.1. Infrared spectra

In compound $[VO(\mu_2\text{-}OCH_3)(L^1)]_2$ (**1**), a strong intensity bands observed with splittings at 1600 and 1547 cm^{-1} are due to newly formed —C=N—N=C— moiety. A weak band observed at 1718 cm^{-1} is assigned to the acetylacetonto C=C band. The dinuclear complex exhibits a sharp band at 980 cm^{-1} due to ν(V=O) and a broad but sharp band at 895–944 cm^{-1} due to ν[V–(μ-O)–V] mode.

In IR spectrum of complex **2** exhibits a broad band at 3450 cm^{-1} due to hydrogen bonded N—H of pyridinium group and O—H of water molecule. The —C=N—N=C— moiety is observed as a medium band at 1618 and 1589 cm^{-1}. The complex **2** shows strong bands at around 997 and 859 cm^{-1} which may be assigned to antisymmetric and symmetric ν(O=V=O) vibrations of the *cis*-VO_2 group, respectively [10]. The spectrum shows ν(C=C, C=N) vibrations in the range 1399–1618 for **2**. A band around 1719 cm^{-1} is probably due to ν(C=C) of acetylacetonato moiety.

In the compound **3**, NH_2 shows two bands at 3304 and 3145 cm^{-1}. The —C=N—N=C— moiety is observed as medium bands at 1598–1638 cm^{-1}. The very strong band at 938 cm^{-1} and weak band at 980 cm^{-1} are assigned to ν(V=O) of dioxo. ν(CS) appears at 810 cm^{-1}.

3.2. Electronic spectra

The isolated complexes are usually dark in appearance and are soluble in polar protic solvents but sparingly soluble in common organic solvents. The electronic spectrum of ligand HL^3 in methanol showed the $\pi \rightarrow \pi^*$ and $n \rightarrow \pi^*$ transitions at 201 and 314 nm, respectively. For the complexes **1**, **2** and **3**, no d–d bands are expected as there are no d electrons. Compounds **1**, **2** and **3** display an intense electronic spectral band in the near-UV region, Fig. 1. This band originates due to ligand to metal charge transfer (LMCT) transition. The values are 345 nm for **1**, 354 for **2** and 420 nm for **3**. The other bands observed at 271 and 214 nm for **1**, 274 and 208 nm for **2**, 312 and 210 nm for **3** correspond mainly to intraligand transitions. DFT calculations on the similar hydrazone complex show that LMCT transitions contribute also in the other bands [35]. The LMCT energy of complexes derived from Schiff base ligands decreases in the order: **1** > **2** > **3**. The intense 208–214 nm and 271–312 nm bands were assigned to intraligand $\pi \rightarrow \pi^*$ and $n \rightarrow \pi^*$ transitions, respectively [35,36].

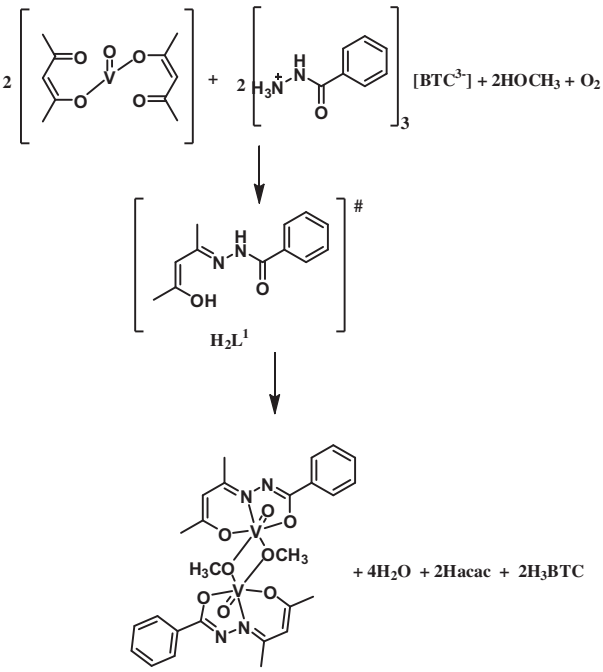

Scheme 2. Synthesis pathway of **1**.

3.3. ^1H NMR spectra

^1H NMR data of all the complexes are given in Section 2. The coordinating modes of the ligands were also confirmed by recording ^1H NMR spectra of the complexes in $CDCl_3$ and DMSO-d^6. ^1H NMR signals were assigned on the basis of intensity, chemical shift values and deuteration experiments. The ^1H NMR spectra of all complexes show the simultaneous occurrence of two sets of signals, which are attributable on one hand to the aromatic entities and on the other hand to the aliphatic moiety. Absence of the NH proton in the spectra of the complexes **1** and **2**, suggests the conversion of the keto to the tautomeric enol group and subsequent

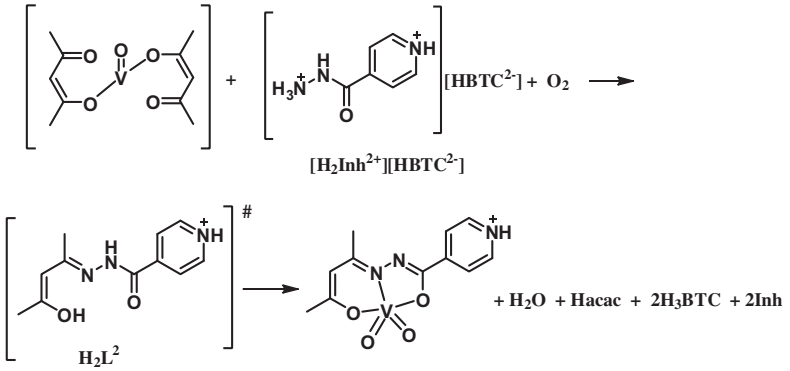

Scheme 3. Synthesis pathway of **2**.

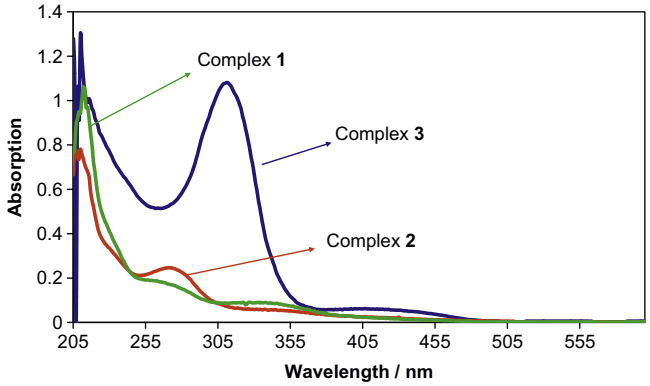

Fig. 1. Electronic spectra of the complexes **1**–**3** in methanol ($c = 2 \times 10^{-5}$ M).

coordination of the enolate oxygen of the aroyl hydrazone Schiff base ligands. Aromatic protons of the complexes appear well within the expected range. The methyl region of the acetylacetonato complexes exhibits two signals for methyl protons of **1** and **2** between 2.4 and 2.7 ppm [37]. Complex $[V^{V}O_2(L^2)]\cdot H_2O$ (**2**) studied both in DMSO-d^6 and $CDCl_3$ solution for solubility reason. Complex $[V^{V}O(\mu_2\text{-}OCH_3)(L^1)]_2$ (**1**) was identified by its NMR spectrum in $CDCl_3$ solution. Apart from all the aromatic proton signals of the coordinated ligand L^2, the spectrum of **1** exhibited one singlet at 5.12 ppm corresponds to protons of the bridging OCH_3 group in addition to another singlet (with different intensity) at 3.49 ppm attributed to the coordinated terminal OCH_3 group [38]. These two peaks indicate that this dimeric species is decomposed to the corresponding monomeric species significantly (the ratio of dimeric species to monomeric being approximately 1:1 in $CDCl_3$

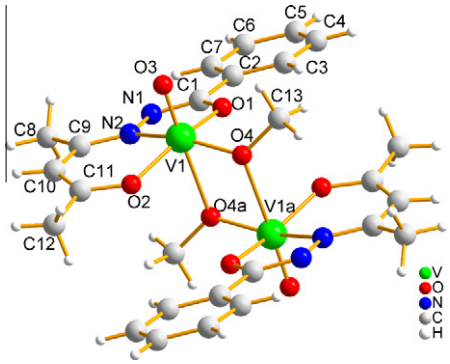

Fig. 2. Molecular structure of **1**. Symmetry code: $a = 1 - x, -y, -z$.

Table 2
Selected bond distances (Å) and angels (°) for complexes **1** and **2**.

Complex **1**[i]		Complex **2**[ii]	
V1–O1	1.9161(12)	V1–O1	1.9352(19)
V1–O2	1.8587(13)	V1–O2	1.9626(18)
V1–O3	1.5868(14)	V1–O3	1.6255(14)
V1–O4	1.8277(12)	V1–O3a	1.6255(14)
V1–N2	2.0830(15)	V1–N1	2.111(2)
V1–O4a	2.3752(12)		
O1–V1–O2	153.59(6)	O1–V1–O2	157.65(8)
O1–V1–O3	98.87(6)	O1–V1–O3	96.67(6)
O1–V1–O4	88.86(5)	O1–V1–N1	82.64(8)
O1–V1–N2	75.02(5)	O1–V1–O3a	96.67(6)
O1–V1–O4a	81.35(5)	O2–V1–O3	96.18(6)
O2–V1–O3	100.37(6)	O2–V1–N1	75.01(8)
O2–V1–O4	104.01(5)	O2–V1–O3a	96.18(6)
O2–V1–N2	84.41(6)	O3–V1–N1	125.16(5)
O2–V1–O4a	80.24(5)	O3–V1–O3a	109.46(7)
O3–V1–O4	103.34(6)	O3a–V1–N1	125.16(5)
O3–V1–N2	98.34(6)		
O3–V1–O4a	177.43(6)		
O4–V1–N2	154.74(6)		
O4–V1–O4a	74.09(5)		
O4a–V1–N2	84.20(5)		

[i] Symmetry code: (a) = $1 - x, -y, -z$.
[ii] Symmetry code: (a) = $x, 1/2 - y, z$.

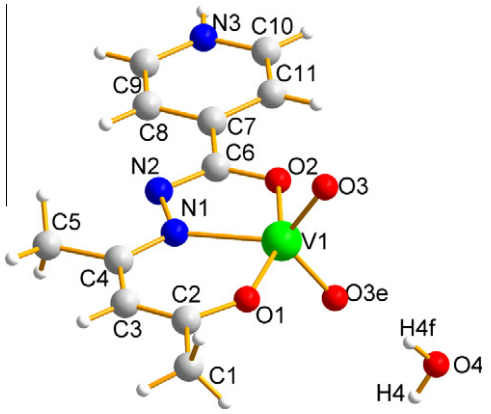

Fig. 3. Molecular structure of $[V^{V}O_2(L^2)]\cdot H_2O$ (**2**). Symmetry codes: (e) = $x, 0.5 - y, z$; (f) = $x, 1.5 - y, z$.

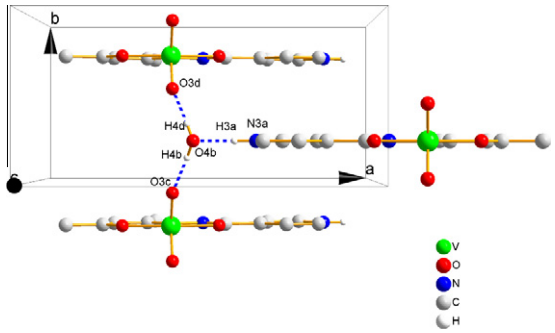

Fig. 4. Crystalline structure of $[V^{V}O_2(L^2)]\cdot H_2O$ (**2**). Hydrogen atoms except those that involved in hydrogen bonding are omitted for clarity. [N(3a)–H(3a)···O(4b) = 2.689(3) Å, N(3a)–H(3a)···O(4b) = 163(3)°], [O(4b)–H(4b)···O(3c) = 2.737(2) Å, O(4b)–H(4b)···O(3c) = 171(2)°]. Symmetry operations used: (a) $1 + x, y, 1 + z$; (b) $0.5 - x, 1 - y, 0.5 + z$; (c) $0.5 - x, -y, 0.5 + z$; (d) $0.5 - x, 0.5 + y, 0.5 + z$.

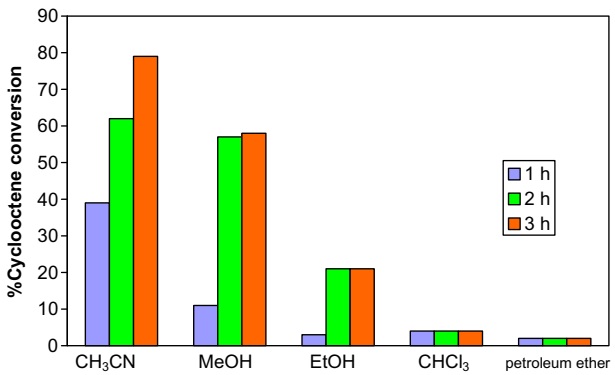

Fig. 5. Effect of solvent in oxidation of cyclooctene with $[V^{V}O_2(L^2)]/H_2O_2$. *Reaction conditions*: $[V^{V}O_2(L^2)]\cdot H_2O$ (**2**) 3 μmol, cyclooctene 1 mmol, chlorobenzene 0.1 g, acetonitrile 2 ml, H_2O_2 3 mmol and temperature 80 ± 1 °C.

solution). Methyls and =CH— protons of the acetylacetonate group also showed doubling of signals (see Section 2) which are attributable to respective monomeric species.

3.4. Description of the structures

The dimeric complex **1**, which lies on a crystallographic center of symmetry is formed by two bridging methoxide-O atoms with V–O(4) and V–O(4a) [symmetry code $a = 1 - x, -y, -z$] bond lengths of 1.8277(12) and 2.3752(12) Å, respectively. The molecular structure of **1** is illustrated in Fig. 2 and the bond parameters are listed in Table 2. The lattice is orthorhombic in nature with *Pbca* symmetry and the unit cell consists of four molecules. The centrosymmetric dimer is formed via the bridging methoxylatos connecting two vanadium atoms. Hence the vanadium atom adopts a distorted octahedral geometry. The V···V separation is 3.3708(1) Å and the angle V1–O4–V1a is 105.912(1)° which is very similar to reported dimethoxy-bridged hydrazone complexes [39–41]. The H_2L^1 ligand binds the vanadium meridionally in its fully deprotonated $(L^1)^{2-}$ form through the acetonate-O of acac, imine-N and deprotonated amide-O in its enol form generating a folded 6-membered and an almost planar 5-membered chelate ring. The corresponding bite angles are 84.41(6)° and 75.02(5)° which are very similar with other reported hydrazone complexes [42,43]. So, the acetonate-O, enolate-O and the imine-N atoms of $(L^1)^{2-}$ species and the methoxide-O atom (lying *trans* to the imine-N) form the square plane with an r.m.s. deviation of 0.0440 Å. Two axial positions are occupied by the oxido-O(3) atom and a bridging

Table 3
Oxidation of various hydrocarbons with $[V^{V}O(\mu_2\text{-}OCH_3)(L^1)]_2$ using H_2O_2 and acetonitrile[a].

Entry	Substrate	Product(s)	Yield (%)[b]	Conv. (%)[b] (time/h)	TON[c]
1		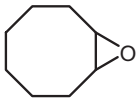	93	94 (4 h)	292
2		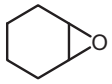	24	100 (5 h)	314
		2-Cyclohexen-1-ol	55		
		2-Cyclohexen-1-one	21		
3		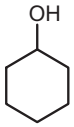	69	97 (5 h)	308
		Cyclohexanone	28		
4		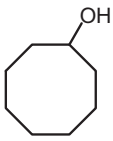	44	87 (5 h)	274
		Cyclooctanone	43		
5	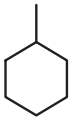	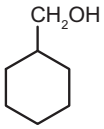	92	92 (5 h)	289
6	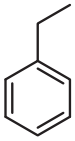	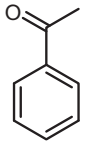	5	5 (4 h)	16
7	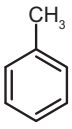	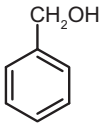	11	11 (1 h)	35
8	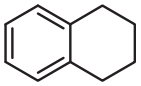	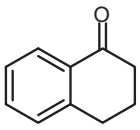	67	67 (5 h)	211

[a] *Reaction conditions*: catalyst 1.60 μmol, substrate 1 mmol, chlorobenzene 0.1 g, acetonitrile 2 ml, H_2O_2 3 mmol and temperature 80 ± 1 °C.
[b] Yields and conversions based on the starting substrate and determined by GC.
[c] TON: turnover number = number of moles of product formed per mole of V in the catalyst.

methoxide-O(4a) atom of the neighboring molecule. The disposition of the oxovanadium groups is anti-coplanar which is also observed in other dimeric oxovanadium complexes [40]. The V=O distance is only 1.5868(14) Å which is very closed to another reported complex [44]. The five V—O bond lengths follow the order: V—O(oxo) < V—O(methoxide)^{e} (e = equaterial) < V—O(acetonato) < V–O(enolate) < V—O(methoxide)^{a} (a = axial).

The compound **2** was synthesized in situ by template method and $[V^{V}O_2(L^2)]\cdot H_2O$ crystallized as a dioxovanadium species due to aerial oxidation into an orthorhombic lattice with *Pnma* symmetry. Suitable crystals for X-ray diffraction were grown from the reaction mixture by branched-tube method in a mixture of ethanol and water (1:1 v/v). The in situ formed ligand H_2L^2 deprotonates and acts as a dianionic tridentate chelating species. It should be noted that since pyridyl nitrogen N3 protonates and forms pyridinium, this leads to a total charge of −1 for the ligand L^2. The molecular structure of the dioxocomplex **2** along with the atom labels is given in Fig. 3. The complex present five-coordinated vanadium(V) center bonded to two oxo ligands in a *cis* arrangement, one nitrogen atom and two oxygen atoms from L^2 (in enol form), which coordinates dianionic in the O,N,O-tridentate mode, forming 5- and 6-membered chelate rings around the vanadium atom. Dioxovanadium(V) complexes with planar tridentate ligands can have either trigonal-bipyramidal or square pyramidal geometry [45,46,25]. Bond lengths and angles of special interest are given in Table 2. The geometry around V1 remains between trigonal-bipyramidal and square planar ($\tau = 0.5415$) [47]. The geometry around the vanadium center is better defined as considerably

Table 4
Oxidation of various hydrocarbons with $[V^{V}O_2(L^2)]$ using H_2O_2 and acetonitrile[a].

Entry	Substrate	Product(s)	Yield (%)[b]	Conv. (%)[b] (time/h)	TON[c]
1		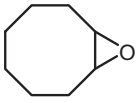	96	96 (5 h)	307
2		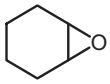	17	93 (3 h)	294
		2-Cyclohexen-1-ol	60		
		2-Cyclohexen-1-one	16		
3		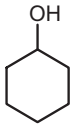	50	89 (5 h)	284
		Cyclohexanone	39		
4		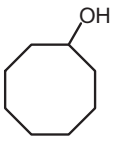	56	88 (5 h)	281
		Cyclooctanone	32		
5	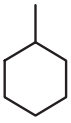	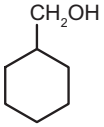	65	65 (5 h)	208
6	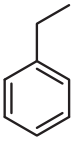	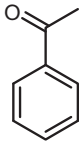	10	10 (5 h)	32
7	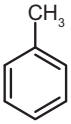	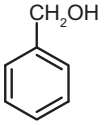	49	49 (5 h)	157
8	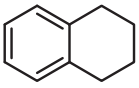	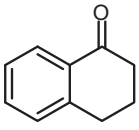	83	83 (1 h)	140

[a] *Reaction conditions*: catalyst 3.13 μmol, substrate 1 mmol, chlorobenzene 0.1 g, acetonitrile 2 ml, H_2O_2 3 mmol and temperature 80 ± 1 °C.
[b] Yields and conversions based on the starting substrate and determined by GC.
[c] TON: turnover number = number of moles of product formed per mole of V in the catalyst.

distorted trigonal bipyramid [48,49]. Two oxo groups and the imine-N atom of L^{2-} form the equatorial plane. Two axial sites are taken up by two oxygen atoms of L^{2}. The V=O distance V1—O3 1.6255(14) is not exceptional [50]. The C(6)–O(2) bond length due to deprotonation extends to 1.306(3) Å in the complex from 1.232(3) Å in the keto form of the analog benzoyl hydrazone ligand [31], making the V(1)–O(2) distance, 1.9626(18) Å.

In the complex **2**, the crystal is stabilized by a net of intermolecular hydrogen bonds, which are shown in Fig. 4. Strong N–H···O and O–H···O hydrogen bonds are found. The nitrogen atom N(3a), of the pyridinium N—H group, is H-bonded through H(3) to the O(4b) atom of water, while H(4) interacts with the vanadyl oxygen atom O(3d) of a second and third complex molecules. By hydrogen bonds $[V^{V}O_2(L^2)]$·molecules are connected together through water molecules and form a chain along *b* axis. The chains are connected along *a* axis by O(4b)···N(3a) hydrogen bonds.

3.5. Catalytic reactivity

The main driving force for the development of new efficient oxygenation catalysts is the necessity to functionalize feedstock hydrocarbons to raw oxygen-containing chemicals and the ability to selectively hydroxylate non-activated C—H bonds in elaborate chemicals in order to save many steps in the preparation of fine chemicals. In addition, for obvious environmental constraints, classical stoichiometric oxidants, such as dichromate or permanganate,

Table 5
Oxidation of various hydrocarbons with $[VO_2(L^3)]$ using H_2O_2 and acetonitrile[a].

Entry	Substrate	Product(s)	Yield (%)[b]	Conv. (%)[b] (time/h)	TON[c]
1		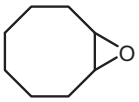	96	94 (5 h)	265
2		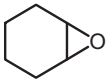	31	98 (2 h)	271
		2-Cyclohexen-1-ol	52		
		2-Cyclohexen-1-one	15		
3		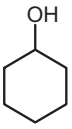	48	87 (4 h)	240
		Cyclohexanone	39		
4		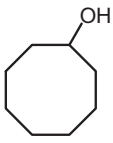	71	100 (5 h)	276
		Cyclooctanone	29		
5	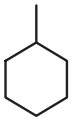	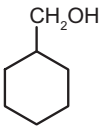	86	86 (5 h)	238
6	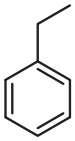	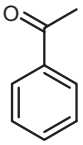	71	71 (5 h)	196
7	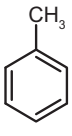	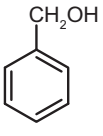	31	31 (5 h)	86
8	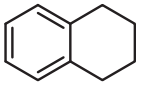	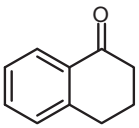	63	63 (1 h)	174

[a] *Reaction conditions*: catalyst 3.62 μmol, substrate 1 mmol, chlorobenzene 0.1 g, acetonitrile 2 ml, H_2O_2 3 mmol and temperature 80 ± 1 °C.
[b] Yields and conversions based on the starting substrate and determined by GC.
[c] TON: turnover number = number of moles of product formed per mole of V in the catalyst.

should be replaced by new environment friendly catalytic processes using clean oxidants like molecular oxygen or hydrogen peroxide [51,52].

The catalytic oxidation of cyclooctene with hydrogen peroxide was studied in the presence of $[V^{V}O_2(L^2)]\cdot H_2O$ (**2**). All reactions were carried out with 1 mmol of cyclooctene in CH_3CN and in the presence of catalyst **2** at 80 °C. Cyclooctene oxide was the sole product. The results of control experiments revealed that the presence of catalyst and oxidant are essential for the oxidation. The oxidation of cyclooctene in the absence H_2O_2 does not occur and in the absence of catalyst the oxidation proceeds only up to 6% after 24 h.

In search of suitable reaction conditions to achieve the maximum oxidation of cyclooctene, the effect of solvent was studied. Fig. 5 illustrates the influence of the solvent nature in the catalytic epoxidation of cyclooctene by **2**. Methanol, ethanol, acetonitrile, chloroform and petroleum ether were used as solvents. The highest conversion was obtained in acetonitrile, 79% after 3 h. It was observed that the catalytic activity of complex **2** decreases in order acetonitrile (relative dielectric constants [53], $\varepsilon/\varepsilon_0 = 37.5$) > methanol (32.7) > ethanol (26.6) > chloroform (4.9) > petroleum ether (≈2). In Fig. 5, the solvents are shown in order of their relative dielectric constants ($\varepsilon/\varepsilon_0$). In general, there was a good correlation between the solvent polarity ($\varepsilon/\varepsilon_0$) and cyclooctene conversion percent. The highest conversion in acetonitrile possibly is caused by its high dielectric constant.

The catalytic activities of **1**–**3** were examined in oxidation of various hydrocarbons under the optimized conditions (H_2O_2/cyclooctene molar ratio = 3, acetonitrile, reaction temperature 80 °C) and the results are shown in Tables 3–5. Cyclooctene was converted to the corresponding epoxide with 100% selectivity. For cyclohexene in addition to cyclohexene oxide, allylic oxidation products (2-cyclohexene-1-ol and 2-cyclohexene-1-one) were also formed. Allylic oxidation has been reported in the metalloporphyrin systems [54,55] in the oxidation of alkenes such as cyclohexene and represents radical nature of the active oxidizing species.

Catalysts **1**–**3** oxidized various cyclic alkanes including cyclohexane, cyclooctane and methylcyclohexane to the corresponding alcohol and/or ketone with conversions 87–97% for **1**, 65–89% for **2** and 86–100% for **3** (Tables 3–5). The profile of products show the oxidation reaction is highly selective. The oxidation of tertiary and secondary carbon atoms is favored electronically but the only product of methylcyclohexane oxidation was cyclohexylmethanol by the three catalysts. This finding shows that the reaction products are controlled mainly by steric effects not electronic one. Catalysts **1**–**3** were also active in oxidation of aromatic toluene, ethylbenzene and tetrahydronaphthalene (Tables 3–5). The highest conversion (63–83%) was observed for tetrahydronaphthalene and the lowest for ethylbenzene (5–71%) by catalyst **1**–**3**. Electron-rich alkenes and alkanes displayed a greater activity than aromatic compounds. Hydrocarbons with electron withdrawing phenyl substituent showed a lower product yield and turnover number than the electron rich ones (Table 3–5, entries 6–8).

Catalytic activities of three catalysts **1**–**3** are compared in Fig. 6. In general, electronic and steric effects of the ligands L^{1-3} are almost the same and the catalysts show nearly the same reactivity towards various hydrocarbons except tetralene and cyclohexene. These findings (Fig. 6) suggest the plausible presence of some type of interactions between tetralene and the catalyst **2** that reinforce its approach to the catalyst and fast oxidation (Fig. 6). Such situation is also seen for the catalyst **3** in the oxidation of cyclohexene. Conclusive interpretation of this subject needs further studies in the future. The total mechanism of the reaction is not fully clear. However, on the basis of the oxidation products of the various hydrocarbons (Tables 3–5), it is predicted that the oxidation reactions proceed by intermediacy of a peroxo-vanadium-hydrazone Schiff base species formed in the reaction mixture in the presence of hydrogen peroxide [38].

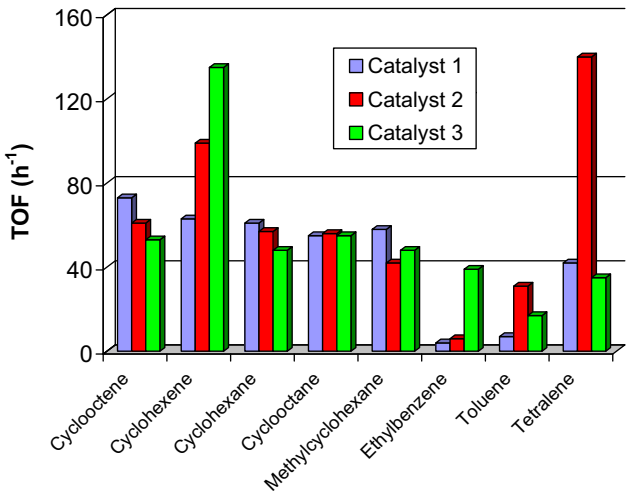

Fig. 6. Comparison of catalytic activities of catalysts **1**–**3** in oxidation of various hydrocarbons with hydrogen peroxide. TOF: turnover frequency = the catalytic turnover per unit time.

4. Conclusions

Our work has revealed that oxo- and dioxovanadium(V) complexes of tridentate hydrazone Schiff base ligands could be synthesized by a proton-transfer complex of hydrazide. Two new oxo- and dioxo-vanadium(V) complexes of hydrazone ONO donor ligands with the formula $[V^{V}O(\mu_2\text{-}OCH_3)(L^1)]_2$ (**1**) and $[V^{V}O_2(L^2)]\cdot H_2O$ (**2**) were synthesized by this method and characterized by spectroscopic and single crystal X-ray analyses. The catalytic abilities of complexes **1**–**3** were investigated by using the environmentally benign and clean oxidant H_2O_2 for oxidation of various hydrocarbons. Alcohol and/or ketone were obtained with good to excellent conversion as the main products of the hydrocarbon oxidation.

Acknowledgements

The authors are grateful to the Zanjan University, the Faculty of Chemistry and Biochemistry of the Ludwig-Maximilians-Universität München, and the School of Chemistry for financial assistance.

Appendix A. Supplementary data

CCDC 801668, 801669, and 669245 contain the supplementary crystallographic data for **1**, **2**, and **3**. These data can be obtained free of charge via http://www.ccdc.cam.ac.uk/conts/retrieving.html, or from the Cambridge Crystallographic Data Centre, 12 Union Road, Cambridge CB2 1EZ, UK; fax: (+44) 1223-336-033; or e-mail: deposit@ccdc.cam.ac.uk.

References

[1] J.A. Littlechild, E. Garcia-Rodriguez, Coord. Chem. Rev. 237 (2003) 65.
[2] S. Macedo-Ribeiro, W. Hemrika, R. Renirie, R. Wever, A. Messerschmidt, JBIC, J. Biol. Inorg. Chem. 4 (1999) 209.
[3] D. Rehder, Inorg. Biochem. 80 (2000) 133.
[4] A.A. Antipov, D.Y. Sorokin, N.P. L'Vov, J.G. Kuenen, Biochem. J. 369 (2003) 185.
[5] M.R. Maurya, Coord. Chem. Rev. 237 (2003) 163.
[6] R.R. Eady, Coord. Chem. Rev. 237 (2003) 23.
[7] W. Plass, Angew. Chem., Int. Ed. Engl. 38 (1999) 909.
[8] D. Rehder, Bioinorganic Vanadium Chemistry, John Wiley and Sons Ltd., 2008.

[9] H. Sakurai, Y. Kojima, Y. Yoshikawa, K. Kawabe, H. Yasui, Coord. Chem. Rev. 226 (2002) 187.
[10] A.M.B. Bastos, J.G. da Silva, P.I.S. Maia, V.M. Deflon, A.A. Batista, A.V.M. Ferreira, L.M. Botion, E. Niquet, H. Beraldo, Polyhedron 27 (2008) 1787.
[11] P. Noblía, M. Vieites, B.S. Parajn-Costa, E.J. Baran, H. Cerecetto, P. Draper, M. González, O.E. Piro, E.E. Castellano, A. Azqueta, A.L. Ceráin, A. Monge-Vega, D. Gambino, J. Inorg. Biochem. 99 (2005) 443.
[12] D.C. Crans, J.J. Smee, E. Gaidamauskas, L. Yang, Chem. Rev. 104 (2004) 849.
[13] S. David, V. Barros, C. Cruz, R. Delgado, FEMS Microbiol. Lett. 251 (2005) 119.
[14] L.H. Terra, A.M.C. Areias, I. Gaubeur, M.E.V. Suez-Iha, Spectrosc. Lett. 32 (1999) 257.
[15] M.R. Maurya, S. Agarwal, M. Abid, A. Azam, C. Bader, M. Ebel, D. Rehder, Dalton Trans. (2006) 937.
[16] M. Mohan, M.P. Gupta, L. Chandra, N.K. Jha, Inorg. Chim. Acta 151 (1988) 61.
[17] A.C. Cunha, J.M. Figueiredo, J.L.M. Tributino, A.L.P. Miranda, H.C. Castro, R.B. Zingali, C.A.M. Fraga, M.C.B.V. Souza, V.F. Ferreira, E.J. Barreiro, Bioorg. Med. Chem. 11 (2003) 2051.
[18] J.P. Mahy, S. Gaspard, D. Mansuy, Biochemistry 32 (1993) 4014.
[19] P.I.S. Maia, F.R. Pavan, C.Q.F. Leite, S.S. Lemos, G.F. de Sousa, A.A. Batista, O.R. Nascimento, J. Ellena, E.E. Castellano, E. Niquet, V.M. Deflon, Polyhedron 28 (2009) 398.
[20] T. Hirao, T. Fujii, T. Tanaka, Y. Oshiro, J. Chem. Soc., Perkin Trans. 1 (1994) 3.
[21] V. Conte, F.D. Furia, G. Licini, Appl. Catal., A 157 (1997) 335.
[22] E. Kwiatkowski, G. Romanowski, W. Nowicki, M. Kwiatkowski, K. Suwińska, Polyhedron 26 (2007) 2559.
[23] V. Vergopoulos, W. Priebsch, M. Fritzsche, D. Rehder, Inorg. Chem. 32 (1993) 1844.
[24] X. Li, M.S. Lah, V.L. Pecoraro, Inorg. Chem. 27 (1988) 4657.
[25] C.A. Root, J.D. Hoeschele, C.R. Cornman, J.W. Kampf, V.L. Pecoraro, Inorg. Chem. 32 (1993) 3855.
[26] B.J. Hamastra, G.J. Kolpas, V.L. Pecoraro, Inorg. Chem. 37 (1998) 949.
[27] N. Julien-Cailhol, E. Rose, J. Vaisserman, D. Rehder, J. Chem. Soc., Dalton Trans. (1996) 2111.
[28] K.H. Thompson, C. Orvig, Coord. Chem. Rev. 1033 (2001) 219.
[29] I.W.C.E. Arends, M.P. Birelli, R.A. Sheldon, Stud. Surf. Sci. Catal. 110 (1997) 1031.
[30] T.S. Smith II, V.L. Pecoraro, Inorg. Chem. 41 (2002) 6750.
[31] O. Pouralimardan, A.-C. Chamayou, C. Janiak, H. Hosseini-Monfared, Inorg. Chim. Acta 360 (2007) 1599.
[32] A. Altomare, M.C. Burla, M. Camalli, G.L. Cascarano, C. Giacovazzo, A. Guagliardi, A.G.G. Moliterni, G. Polidori, Appl. Crystallogr. 32 (1999) 115.
[33] G.M. Sheldrick, Acta Crystallogr., Sect. A 64 (2008) 112.
[34] DIAMOND (Version 3.0) for Windows, Crystal Impact Gbr, Bonn, Germany, 2004, Available from: <http://www.crystalimpact.com/diamond>.
[35] H. Hosseini Monfared, S. Alavi, R. Bikas, M. Vahedpour, P. Mayer, Polyhedron 29 (2010) 3355.
[36] R.M. Silverstein, G.C. Bassler, T.C. Morrill, Spectrometric Identification of Organic Compounds, John Wiley and Sons, New York, 1981.
[37] R. Bikas, H. Hosseini Monfared, S. Alami, I. Pantenburg, G. Meyer, Z. Naturforsch. 65b (2010) 1457.
[38] H. Hosseini Monfared, R. Bikas, P. Mayer, Chim. Acta 363 (2010) 2574.
[39] C. Tsiamis, B. Voulgaropoulos, D. Charistos, G.P. Voutsas, C.A. Kavounis, Polyhedron 19 (2000) 2003.
[40] Z.-P. Deng, S. Gao, L.H. Huo, H. Zhao, Acta Crystallogr., Sect. E 61 (2005) m2214.
[41] B. Mondal, M.G.B. Drew, R. Banerjee, T. Ghosh, Polyhedron 27 (2008) 3197.
[42] M.R. Maurya, S. Agarwal, C. Bader, M. Ebel, D. Rehder, Dalton Trans. (2005) 537.
[43] S.P. Rath, S. Mondal, A. Chakravorty, Inorg. Chim. Acta 263 (1997) 247.
[44] M. Moon, M. Pyo, Y.C. Myoung, C.I. Ahn, M.S. Lah, Inorg. Chem. 40 (2001) 554.
[45] S.N. Pal, K.R. Rahika, S. Pal, Z. Anorg. Allg. Chem. 627 (2001) 1631.
[46] A.G.J. Ligtenbarg, A.L. Spek, R. Hage, B.L. Feringa, J. Chem. Soc., Dalton Trans. (1999) 659.
[47] τ = (difference between the two largest angles)/60 for five coordinated metal centers allows for the distinction between trigonal-bipyramidal (ideally $\tau = 1$) and square-pyramidal (ideally $\tau = 0$): A.W. Addison, T.N. Rao, J. Reedijk, J. van Rijnn, G.C. Verschoor, J. Chem. Soc., Dalton Trans. (1984) 1349.
[48] L.M. Mokry, C.J. Carrano, Inorg. Chem. 32 (1993) 6119.
[49] E. Kwiatkowski, G. Romanowski, W. Nowicki, M. Kwiatkowski, K. Suwińska, Polyhedron 22 (2003) 1009.
[50] M.R. Maurya, A. Kumar, A.R. Bhat, A. Azam, C. Bader, D. Rehder, Inorg. Chem. 45 (2006) 1260.
[51] H. Hosseini Monfared, Z. Amouei, Mol. Catal. A: Chem. 217 (2004) 161.
[52] I.W.C.E. Arends, R.A. Sheldon, Top. Catal. 19 (2002) 133.
[53] Y. Marcus, in: J. Rydberg, C. Musikas, G.R. Choppin (Eds.), Principles and Practices of Solvent Extraction, Marcel Dekker, New York, 1992, p. 23.
[54] D. Mohajer, H. Hosseini Monfared, J. Chem. Res. (1998) 772.
[55] A.J. Appleton, S. Evans, J.R. Lindsay Smith, J. Chem. Soc., Perkin Trans. 2 (1996) 281.